NEURAL REGENERATION RESEARCH
www.nrronline.org

Research Article

Hypothermia selectively protects the anterior forebrain mesocircuit during global cerebral ischemia

https://doi.org/10.4103/1673-5374.330616
Date of submission: February 4, 2021
Date of decision: May 5, 2021
Date of acceptance: October 11, 2021
Date of web publication: December 10, 2021

Xiao-Hua Wang[1, 2, #], Wei Jiang[3, #], Si-Yuan Zhang[4], Bin-Bin Nie[5, 6], Yi Zheng[7], Feng Yan[8], Jian-Feng Lei[8], Tian-Long Wang[1, 2, *]

From the Contents

Graphical Abstract *Hypothermia reduces the hypometabolic regions of rats with global cerebral ischemia*

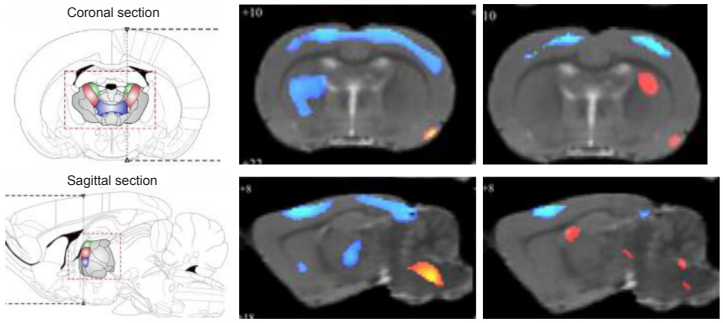

Abstract

Hypothermia is an important protective strategy against global cerebral ischemia following cardiac arrest. However, the mechanisms of hypothermia underlying the changes in different regions and connections of the brain have not been fully elucidated. This study aims to identify the metabolic nodes and connection integrity of specific brain regions in rats with global cerebral ischemia that are most affected by hypothermia treatment. ^{18}F-fluorodeoxyglucose positron emission tomography was used to quantitatively determine glucose metabolism in different brain regions in a rat model of global cerebral ischemia established at 31–33°C. Diffusion tensor imaging was also used to reconstruct and explore the brain connections involved. The results showed that, compared with the model rats established at 37–37.5°C, the rat models of global cerebral ischemia established at 31–33°C had smaller hypometabolic regions in the thalamus and primary sensory areas and sustained no obvious thalamic injury. Hypothermia selectively preserved the integrity of the anterior forebrain mesocircuit, exhibiting protective effects on the brain during the global cerebral ischemia. The study was approved by the Institutional Animal Care and Use Committee at Capital Medical University (approval No. XW-AD318-97-019) on December 15, 2019.

Key Words: anterior forebrain mesocircuit; cardiac arrest; corpus callosum; global cerebral ischemia; hypometabolic areas; hypothermia; magnetic resonance imaging; positron emission tomography; prefrontal cortex; rats; thalamus

Chinese Library Classification No. R454.5; R743; R318.52

Introduction

Cumulative evidence has shown that hypothermia provides protection of cerebral function, especially in global cerebral ischemia (GI) following cardiac arrest (CA) (Massaro et al., 2013; Randhawa et al., 2015). In the renewed guidelines, therapeutic hypothermia (TH) was the recommended care for post-CA in comatose survivors of CA (Nguyen et al., 2018). The outcomes of CA have improved in the era of TH management (Larribau et al., 2018; Nguyen et al., 2018). Ninety-two percent of patients experience a return to normal or near-normal neurological function (Mooney et al., 2011). Clinical results have provided strong evidence that hypothermia effectively improved the outcomes in patients with CA, stroke or traumatic brain injury (Wu and Grotta, 2013; Kowalik et al., 2014; Wu et al., 2016). Two large randomized controlled trials reported that 32–34°C hypothermia for 24 hours reduced epilepticus seizure (Legriel et al., 2016), and that hypothermia after cardiopulmonary resuscitation resulted in no or minor brain dysfunction (Arrich et al., 2016). On the basis of the importance of hypothermia in GI, previous studies have investigated its underlying cerebral protective mechanisms based on the associated RNA, protein and cytokine levels (Han et al., 2012; Park et al., 2013; Carlin et al., 2017; Wang et al., 2018; Font-Belmonte et al., 2020). Hypothermia also protects

[1]Department of Anesthesiology, Xuanwu Hospital, Capital Medical University, Beijing, China; [2]National Clinical Research Center for Geriatric Disorders, Beijing, China; [3]Department of Anesthesiology, Third Medical Center of People's Liberation Army General Hospital, Beijing, China; [4]Daxing Hospital Affiliated to Capital Medical University, Beijing, China; [5]Beijing Engineering Research Center of Radiographic Techniques and Equipment, Institute of High Energy Physics, Chinese Academy of Sciences, Beijing, China; [6]School of Nuclear Science and Technology, University of Chinese Academy of Sciences, Beijing, China; [7]Neuroprotection Research Laboratory, Departments of Radiology and Neurology, Massachusetts General Hospital and Harvard Medical School, Charlestown, MA, USA; [8]Cerebrovascular Research Center, Xuanwu Hospital, Capital Medical University, Beijing, China
*Correspondence to: Tian-Long Wang, PhD, w_tl5595@yahoo.com.
https://orcid.org/0000-0003-1636-0142 (Tian-Long Wang)
#Both authors contributed equally to this work.

Funding: *This study was supported by Beijing Municipal Health Commission of China, No. Jing2019-2 (to TLW).*
How to cite this article: *Wang XH, Jiang W, Zhang SY, Nie BB, Zheng Y, Yan F, Lei JF, Wang TL (2022) Hypothermia selectively protects the anterior forebrain mesocircuit during global cerebral ischemia. Neural Regen Res 17(7):1512-1517*

the neuronal mitochondria as well as the neurovascular unit in GI (Liu et al., 2016; Carlin et al., 2017; Tang et al., 2020). In a prospective multi-center large cohort study on hypothermia, proton magnetic resonance imaging (MRI) of the thalamus (Ts) showed a clear reduction in incidence of natal encephalopathy (Lally et al., 2019). Three large hypothermia trials have shown that hypothermia reduces both the frequency and severity of brain lesions as seen on MRI (Rutherford et al., 2010; Cheong et al., 2012; Shankaran et al., 2012). However, until now, the protective mechanisms of hypothermia in the functional and metabolic activities of special regions, connection nodes and their associated networks have been poorly understood.

In this study, we used ^{18}F-fluorodeoxyglucose positron emission tomography (^{18}F-FDG-PET) to quantitatively determine the glucose metabolism of different regions in the brain. In addition, we used diffusion tensor imaging (DTI) tractography to reconstruct and explore the cerebral connections protected by hypothermia. Our aim was to investigate the metabolic nodes and connection integrity of a specific circuit in a rat model of hypothermia-induced GI to further elucidate the cerebral protective functions of hypothermia.

Materials and Methods

Animal model

The study protocols were approved by the Institutional Animal Care and Use Committee at Capital Medical University (approval No. XW-AD318-97-019) on December 15, 2019. The animals were purchased from Beijing Vital River Laboratory Animal Technology Co. Ltd., affiliated with Charles River Laboratories (CRL), Beijing, China (license No. SCXK 2001-0017), and were housed at the Animal Care Facilities of Capital Medical University. All experiments conformed to the Guide for the Care and Use of Laboratory Animals (National Institutes of Health Publication 85-23, revised in 1985). All experiments were designed and reported according to the Animal Research: Reporting of *In Vivo* Experiments (ARRIVE) guidelines. The animals were housed under controlled environmental conditions (12-hour light/dark cycle, ambient temperature 23 ± 2°C and 60–70% humidity).

This study used male animals only because female animals have higher estrogen levels that protect them from infection. Eighteen male Sprague-Dawley rats, specific-pathogen-free level, 9–11 weeks old, weighing 320–350 g, were randomized into three groups. The hypothermia GI group (n = 6) was maintained at 31–33°C to establish the GI model. The temperature probe was inserted into the rectum and the rats were placed on a cooling/warming blanket (CMA 150, Carnegie Medicine, Stockholm, Sweden) that was connected to a thermostatically controlled system (CMA 150, Carnegie Medicine) that maintained the temperature using feedback regulation. During a 25-minute cooling period, alcohol was sprayed on the fur of rats to reduce body temperature. The hypothermia period was maintained for 150 minutes, after which the rats were warmed for 30 minutes, and then maintained at normal temperature until scanned. The normothermia GI group (n = 6) was maintained at 37–37.5°C using cooling/warming blankets with the same system to establish the GI model. Duration of normothermia was maintained for 150 minutes (**Figure 1**). The sham group (n = 6) was maintained at 37–37.5°C and subjected to a median incision in the neck but without induction of GI model.

The 2-vessel occlusion GI model was accomplished using a modification of the Longa's method, as previously described (Smith et al., 1984; Zhang et al., 2013). Catheters were inserted into the external jugular veins to draw blood, the left femoral artery for blood pressure monitoring and the right femoral artery for Heparin (H12020505, Tianjin Biochem Pharmaceutical Co., Ltd., Tianjin, China) infusion. Under an operating microscope (Perlong Medical Equipment Co., Ltd. Nanjing, China), a median incision in the neck was made and the bilateral common carotid arteries were isolated and each proximally encircled by a ligature line. Heparin (150 IU/kg) was administered and blood was drawn via the jugular catheter to decrease the mean arterial pressure to 40–50 mmHg. During the procedure, the vagus nerve was carefully preserved, blood gases were measured and the tidal volume of the respirator during the intubated period was adjusted to achieve an arterial partial pressure of carbon dioxide of 35–45 mmHg, an arterial partial pressure of oxygen > 90 mmHg and a pH value of 7.35–7.45. After approximately 10 minutes of the left common carotid artery ligature, the right common carotid artery was ligated to finally block the cerebral blood flow. After a total of 15 minutes, the blood was slowly re-infused through the jugular catheter, followed by 0.5 mL sodium bicarbonate (0.6 M). After a 135-minute recovery period, the wounds were sutured and the rats were returned to their cages. No animals or data points were excluded from the analysis.

Data acquisition for ^{18}F-FDG-PET, MRI DTI, and T2

The rats were scanned 24 hours after the GI model was established. Before ^{18}F-FDG injection, all rats had access to drinking water at all times but were deprived of food for 12–15 hours. For each rat, ^{18}F-FDG (18.5 MBq/100 g body weight; Atom High Technology (HTA) Co., Ltd., Beijing, China) was administered via tail vein injection without anesthesia. Subsequently, the rats were returned to their cages and kept in a room for 40 minutes with minimal ambient noise for maximization of ^{18}F-FDG uptake in the brain (Caballero Perea et al., 2012; Quinn et al., 2016). Subsequently, the rats were anesthetized using a nose cone with 2% isoflurane in 100% oxygen (IsoFlo, Hebei Jiumu Pharma, Ltd., Langfang, China) for the period of the scan. The rats were placed in the prone position on the scanner bed and with a plastic stereotactic head holder. ^{18}F-FDG-PET images were acquired on an animal PET system (E-plus260, Institute of High Energy Physics, Chinese Academy of Sciences, Beijing, China) at the center of the field of view and a static acquisition of 10 minutes with radial spatial resolution of 1.55 mm full-width half maximum was performed. The images were subsequently reconstructed using the ordered subsets expectation maximization (4 iterations, 12 subsets) algorithm. They were reconstructed on a 90 matrix × 97 matrix × 200 matrix, with a voxel size of 0.5 × 0.5 × 1 mm^3. Finally, all scans were saved in the analyze format. DTI data were acquired by a 38-mm birdcage rat brain quadrature resonator for radiofrequency transmission using a 7.0 T animal MRI scanner (70/16 PharmaScan, Bruker Biospin GmbH, Rheinstetten, Germany). DTI images were obtained with 12,000 ms repetition time, 32.248 ms echo time, 163 matrix size, DTI image 128 × 128 × 48 mm^3, voxel size 0.35 × 0.35 × 0.56 mm^3, with no slice gap. Diffusion weighting was applied along 30 independent axes, with a b value of 1000 s/mm^2. Eight reference images with a b value of 0 s/mm^2 were acquired. Finally, Paravision 5.0 software programs (Bruker Biospin corporation, Baltimore, MD, USA) converted all original Bruker images to the DICOM format (Li et al., 2016; Zhang et al., 2016).

Analysis of ^{18}F-FDG-PET images

Data analysis of all ^{18}F-FDG-PET images and identification of the significant differences of ^{18}F-FDG signals were performed in a rat statistical parametric mapping (spmrat)-IHEP toolbox (Nie et al., 2013, 2014) in SPM8 (Wellcome, Department of Cognitive Neurology, London, UK). First, using MRIcro manually removed background and the body tissues of all images (Mangin et al., 2016), the origins of the images were repositioned at D3V to correspond to the standard ^{18}F-FDG-PET template (Paxinos and Watson, 2005). By scaling up the

voxel size in the Analyze header, the individual rat brain images were normalized into Paxinos & Watson space spatially by a factor of 4 (Casteels et al., 2006; Nie et al., 2010), registering to the ^{18}F-FDG-PET template, the extracranial tissues were removed via the intracranial image and the background cut off by shearing the matrix. Finally, all normalized ^{18}F-FDG-PET images were smoothened by a Gaussian kernel of 2 × 2 × 4 mm^3 full-width half maximum. Based on the framework of the general linear model, all smoothened data were voxel-wise analyzed. Based on an unbiased scale factor, proportional scaling and intensity normalization were applied to account for global confounders (Crone et al., 2014). Based on a voxel-level height threshold of $P < 0.005$, the brain regions with significant ^{18}F-FDG differences from the sham group were yielded. At the cluster level, false discovery rate correction for multiple comparisons was also conducted. The data were analyzed using voxel-based analysis. According to both the sagittal and transverse sections, the realignment of the internal contour of each tract was also translated. The rat brain atlas stereotaxic coordinates were defined such that the *x*-axis is positive to the right and negative to the left of the midline, the *y*-axis is positive toward the ventral direction and negative to the dorsal direction, and the *z*-axis is positive toward the olfactory bulb relative to the bregma and negative in the direction of the cerebellum. The ^{18}F-FDG uptake was compared between the hypothermia/normothermia GI groups and the sham group. If ^{18}F-FDG uptake of the hypothermia/normothermia GI group was lower than sham group, they will have hypo-metabolic regions that will show the cold pseudo-color, blue. If ^{18}F-FDG uptake of the hypothermia/normothermia GI group was higher than sham group, they will have hyper-metabolic regions that will show the warm pseudo-color, orange. If ^{18}F-FDG uptake of the hypothermia/normothermia GI group equals to that of the sham group, the equal-metabolic regions will show the gray pseudo-color, gray. The KE value represents the size of a cluster, specifically the volume of hypometabolic region (Liang et al., 2017).

Analysis of MRI DTI and T2 images

All DTI images were preprocessed in the FMRIB Software Library (FSL) (http://fmrib.ox.ac.uk/fsl). In brief, head motion and eddy currents were removed using FMRIB's Diffusion Toolbox within FSL. The fractional anisotropy (FA) of each individual tract was then calculated. Subsequently, voxel-wise analyses of FA images were performed in a spmrat-IHEP toolbox (SPM8), which is similar to the FDG-PET data analysis (Nie et al., 2013). In brief, the FA data sets were preprocessed by skull stripping and repositioning of the origin point. Then, the FA images were spatially normalized to an FA template image in Paxinos & Watson space (Paxinos and Watson, 2005) and along with MD images. All these FA images were smoothened as described above. Finally, all smoothened data were voxel-wise analyzed based on the general linear model framework. False discovery rate correction for multiple comparisons was also conducted at the cluster level. The higher FA values indirectly reflected conservation of the white fibers.

Statistical analysis

The statistical analysis was performed in spmrat-IHEP (Wellcome Department of Clinical Neurology, London, UK) as follows. Values of the hypothermia or normothermia GI group were averaged and compared with the sham group. The data were analyzed by two-sample *t*-test. The level of significance was regularly set at $P < 0.05$. Based on the generalized linear model, the statistical analysis model of the smoothed mean normalized uptake values ^{18}F-FDG-PET data was established and the Student's *t*-test analysis was performed based on hypothermia GI and normothermia GI groups. The mn-UV was computed in KE, a measure of the size of the cluster as the voxel numbers in the cluster, which directly reflected the volume of the region (Liang et al., 2017). The T_{max} value is the maximum *t*-value in each cluster; a T_{max} value > 1 indicates a significant difference. Peak coordinates (mm) are the coordinates of the maximum point in Paxinos & Watson space.

Results

Hypothermia reduces the hypometabolic regions in brain of GI rat

PET results showed the hypometabolic regions of whole brain were significantly smaller in the hypothermic GI group when compared with those in the normo-thermic GI group (**Figure 2A** and **B**). When compared with the normothermic GI group, the hypothermia GI group also had significantly smaller hypometabolic regions in the Ts and prefrontal-cortex (PFC) and primary sensory areas (**Figure 3A–D**). These results indicate that hypothermia selectively protects the anterior forebrain (cortical) and Ts (subcortical part) of the mesocircuit under GI.

The voxel-wise analysis results are presented as KE values in **Table 1**. As the center of the anterior forebrain thalamic mesocircuit (Schiff, 2008), the voxel number in the Ts hypometabolic regions was significantly lower in the hypothermia GI group compared with that in the normothermia GI group (**Table 1**). The PFC is an important region of the mesocircuit (Schiff, 2008). The KE value in the PFC region was also significantly lower in the hypothermia GI group than that in the normothermia GI group (**Table 1**). The results show that hypothermia significantly preserved anterior forebrain neuronal metabolic activity.

Table 1 | **The KE value in the rat brain in two groups**

			Stereotaxic coordinates		
Anatomical name	**KE**	T_{Max}	***x***	***y***	***z***
Normothermia global cerebral ischemia group					
Prefrontal cortex	553**	4.2414	–0.7308	3.2066	3.7221
Thalamus	2391**	6.1129	–0.8908	8.389	–13.7979
Corpus callosum	54	4.0773	–1.6465	2.6963	2.2821
Internal capsule	29	3.9995	3.4353	3.1571	2.0421
Sensory cortex	1098*	4.8197	4.1167	2.4048	1.0821
Motor cortex	263	3.8065	3.3049	1.2724	1.8021
Prelimbic cortex	477	4.25	–0.73	3.22	3.48
Tegmentum of pons	3426	6.7024	–0.6268	8.2371	–13.5579
Tegmentum of midbrain	1165	5.8208	–1.9484	6.9627	–4.9179
Hypothermia global cerebral ischemia group					
Prefrontal cortex	71**	6.8144	4.5209	6.976	0.8421
Thalamus	342**	5.8853	–0.7704	7.7274	–12.8379
Corpus callosum	4	3.7947	4.1167	3.573	1.0821
Internal capsule	1	3.9995	3.0772	3.995	–1.0779
Sensory cortex	145*	4.5506	3.4353	3.1571	2.0421
Motor cortex	263	3.8065	3.3049	1.2724	1.8021
Prelimbic cortex	477	12.1443	4.5275	7.4567	0.3621
Tegmentum of pons	3474	6.405	–0.6367	7.8811	–12.8379
Tegmentum of midbrain	1105	5.1026	1.292	6.485	–7.3179

KE: The size of a cluster, in which the number, such as 2391, stands for the voxel numbers in the cluster; T_{max} value: the maximum *t*-value in each cluster. T_{max} value > 1 means significant difference. x: *x*-axis, which is negative to the left of the midline and positive to the right; y: *y*-axis, which is positive to the ventral direction relative to the dorsal direction; z: *z*-axis, which is positive in the direction of the olfactory bulb relative to the bregma and negative in the direction of the cerebellum. *$P < 0.05$, **$P < 0.01$ (two-sample *t*-test).

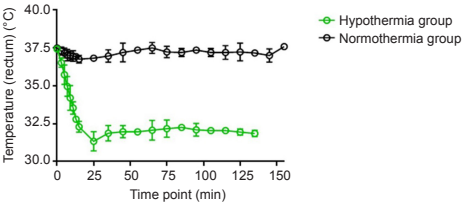

Figure 1 | Rectal temperature during the global cerebral ischemia model procedure.
The rectal temperatures in hypothermia and normothermia global cerebral ischemia groups were 32.5 and 37.5°C, respectively. Data are expressed as the mean ± SD (n = 6). Hypothermia group: Hypothermia global cerebral ischemia group; normothermia group: normothermia global cerebral ischemia group. The rats in the hypothermia cerebral ischemia group were moved to initiate rewarming and the temperature probe was removed from rectum. Therefore, the last two temperatures were not recorded.

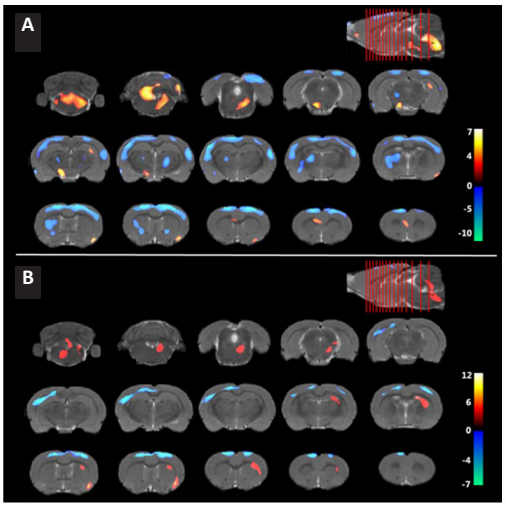

Figure 2 | The hypometabolic regions in the global cerebral ischemia model rats by PET.
(A, B) The hypometabolic regions were significantly larger in the normothermic global cerebral ischemia group (A) when compared with those in the hypothermic global cerebral ischemia group (B). The cold pseudo-color (blue) indicates the hypometabolic regions, while the warm pseudo-color (orange) indicated the hypermetabolic regions. Red lines indicate the position of slice cuts.

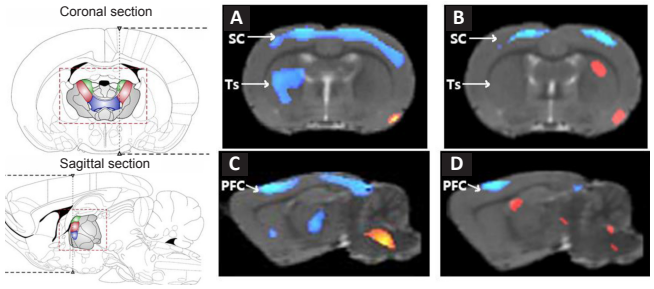

Figure 3 | The hypometabolic regions in anterior forebrain and Ts of the mesocircuit in the global cerebral ischemia model rats.
The hypometabolic regions in the Ts, PFC and primary SC are smaller in the hypothermia GI group than that in the normothermic GI group. The cold pseudo-color (blue) indicates the hypometabolic regions, while the warm pseudo-color (orange) indicates the hypermetabolic regions. (A, B) The coronal sections of the normothermia GI group (A) and hypothermia GI groups (B). (C, D) The sagittal sections of the normothermia GI group (C) and hypothermia GI group (D). GI: Global cerebral ischemia; PFC: prefrontal cortex; SC: sensory cortex; Ts: thalamus.

Hypothermia-treated GI rats have no obvious thalamic injury

The results from the MRI T2 scans show obvious injury to the Ts region in the normothermia GI group (**Figure 4A**). There was almost minimal brain injury in Ts region in the hypothermia GI group (**Figure 4B**).

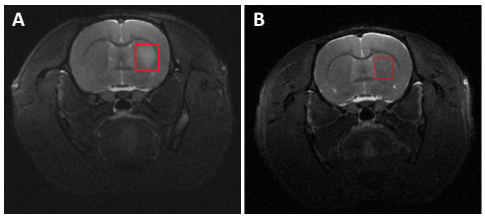

Figure 4 | Difference of brain injury on MRI T2 images between normothermia GI (A) and hypothermia GI (B) groups.
There was obvious damage (red box) to the thalamus in the normothermia GI group. GI: Global cerebral ischemia; MRI: magnetic resonance imaging. Red box indicates the injury part in MRI image.

Difference of connective fibers between hypothermia GI and normothermia GI groups

The DTI MRI indicated the preservation of the corpus callosum and internal capsule (the Ts-cortical white fibers connections) that was also demonstrated by FA in DTI. The voxel-based analysis demonstrated that hypothermia selectively preserved the anterior forebrain mesocircuit, including the Ts, prefrontal cortex (PFC), and the connections including the corpus callosum and internal capsule (**Table 2**).

Table 2 | FA value in the white matter tracts of rat mesocircuit in two groups

Region	Abbreviation	Functional connection	FA value	
			Hypothermia GI group	Normothermia GI group
Internal capsule	IC	Part of the connection between the cortex and thalamus	0.408±0.051*	0.384±0.011
Corpus callosum	CC	Part of the connection between the cortex and thalamus	0.710±0.159**	0.458±0.058
Mammillothalamic tract	MT	Part of the connection between the cortex and thalamus	0.610±0.031	0.670±0.070
Forceps minor of the corpus callosum	FMI	Part of the connection between the cortex and thalamus	0.928±0.071*	0.696±0.121
Forceps major of the corpus callosum	FMJ	Part of the connection between the cortex and thalamus	0.278±0.022	0.191±0.019
Genu of the corpus callosum	GCC	Part of the connection between the cortex and thalamus	0.765±0.147	0.596±0.065
Intermedioventral thalamic commissure	IMVC	Intermedioventral thalamic commissure	0.379±0.062	0.457±0.101
Stria medullaris of the thalamus	SM	Medullaris of the thalamus	0.405±0.209*	0.225±0.064
Longitudinal fasciculus of the pons	LFP	Longitudinal section of the connection between the cortex and thalamus	0.678±0.101	0.528±0.051
Medial forebrain bundle	MFB	Forebrain bundle	0.209±0.013	0.194±0.012
Medial longitudinal fasciculus	MLF	Longitudinal fasciculus	0.894±0.050*	0.661±0.131

Data are expressed as mean ± SD (n = 6). *P < 0.05, **P < 0.01 (two-sample t-test). Cluster number: The number of clusters with consecutive voxels with a significant decrease in FA which is assigned sequentially and artificially. FA: Fractional anisotropy; GI: global ischemia.

Discussion

Our study found that the metabolic activity of the anterior forebrain thalamic mesocircuit and the connective tissue fibers were significantly retained in the hypothermia GI group. GI theoretically produces relatively uniform cellular damage across all brain regions, however, we found that hypothermia produced a graded and differential protection in special neuronal populations and different brain regions in response to global ischemia. Hypothermia significantly preserved anterior forebrain neuronal metabolic activity, as demonstrated by ^{18}F-FDG-PET findings. The MRI T2 results also supported this observation. The preservation of the corpus callosum and internal capsule, the Ts-cortical white fibers connections, was also demonstrated by FA in DTI. The PFC, Ts and associated connections were identified as key components of the anterior forebrain thalamic mesocircuit (Schiff, 2008) and our research identified these areas as those most significantly preserved by hypothermia. That the anterior forebrain mesocircuit was selectively preserved indicates that it plays a pivotal role in hypothermia protection from GI damage.

The anterior forebrain thalamic mesocircuit is the core circuit for maintaining the normal consciousness, arousing and sleep-awake circle (Schiff, 2010; Fridman et al., 2014). This mesocircuit plays a key role in recovery from a coma with potentially retained consciousness and provides the conceptual foundation for the central Ts as the privileged node for arousal neuromodulation (Zhang et al., 2013; Lant et al., 2016). Recent research into the anterior forebrain mesocircuit found that a loss of excitatory output from the central Ts to diffuse cortical areas had a causative role in disorders of consciousness (DOCs) (Lant et al., 2016). In a recent neuroimaging study (Song et al., 2018), selective hypometabolism in the cortex and Ts was reported in acquired DOCs induced by GI injury. Recovery from DOCs has been shown to reverse the modulation of widespread excitation across the anterior forebrain and correlates with the restoration of central thalamic output to the prefrontal cortex (Song et al., 2018). Impairments in the anterior forebrain thalamic mesocircuit appear as DOCs, indicating that this mesocircuit may provide a target for restorative therapies in patients with DOCs (Neske, 2015). Some patients diagnosed as conscious awareness and with cognitive function following severe brain injuries can recover after surprisingly long-time intervals of months, years and even decades (Burruss and Chacko, 1999; Macniven et al., 2003; McMillan and Herbert, 2004; Lammi et al., 2005; Voss et al., 2006). One patient, after remaining in minimally conscious state for 19 years following a severe traumatic brain injury, spontaneously recovered full expressive and receptive language and revealed evidence of ongoing structural rehabilitation (Voss et al., 2006). Forgacs et al. (2016) first described that a patient who underwent prolonged CA and standard TH protocol developed isolation syndrome. This phenomenon was also confirmed in neurological prognostication after CA owing to the recent evolution of clinical practice (Lauritzen et al., 2016). Other recent preclinical studies and pilot clinical studies have reported GI following CA and resuscitation with a standard TH protocol shows isolation syndrome (Owen et al., 2006; Song et al., 2018). The effect of TH on the integrative mesocircuit supports the arousal regulation mechanisms of severe brain injury, even after GI. Structural MRI studies may show structural changes within the brain. Functional, metabolic and structural disconnections within the thalamocortical regions of the default node network lead to unconsciousness and are correlated with the clinical severity. The hypothermia treatment actively modulated the metabolic activity of anterior forebrain mesocircuit.

The anterior forebrain and the Ts are two cardinal structures for the mammalian brain (Granato et al., 1995), and the anterior forebrain mesocircuit is highly conserved in the mammalian brain. Hypothermia selectively preserved the anterior forebrain and the Ts when subjected to limited oxygen and energy conditions during ischemia. The anterior forebrain mesocircuit provides the foundation for the late recovery of function following severe brain injury (Schiff, 2008, 2010). The anterior forebrain mesocircuit may be the important "seed region". Hypothermia selectively protected this region, enabling future recovery and leading to the total recovery of these patients, even several years later. Three possible fundamental pathophysiological mechanisms are likely to account for our findings. First, the highly conserved anterior forebrain mesocircuit has particular neuron and synaptic connections that are different from other neural circuits. Second, that hypothermia leads to the selective protection of special neuronal populations. Third, the anterior forebrain mesocircuit is indispensable for maintaining any hypothermia protection effects (Monti et al., 2015; Boly et al., 2017). The preserved functional integrity of the anterior forebrain provides a specific protective mechanism and potential target for GI treatment.

Nevertheless, there is a caveat that should be considered. We did not test the mesocircuit of female rats with CA conserved following TH. Based on the results in rodents, our next step will be to perform MRI and PET in patients to confirm that this mesocircuit is also preserved by clinically administered hypothermia.

In conclusion, based on ^{18}F-FDG-PET and DTI-MRI findings, we demonstrated that hypothermia can significantly preserve the integrity of the anterior forebrain-thalamic mesocircuit.

Author contributions: *Study design: TLW; PET and MRI data analysis: BBN; data acquisition and interpretation: XHW; study verification: YZ; manuscript draft: WJ; manuscript revision: SYZ. All authors read and approved the final manuscript.*
Conflicts of interest: *The authors declare that the article content was composed in the absence of any commercial or financial relationships that could be construed as a potential conflict of interest.*
Financial support: *This study was supported by Beijing Municipal Health Commission of China, No. Jing2019-2 (to TLW). The funding source had no role in study conception and design, data analysis or interpretation, paper writing or deciding to submit this paper for publication.*
Institutional review board statement: *The study was approved by the Institutional Animal Care and Use Committee at Capital Medical University (approval No. XW-AD318-97-019) on December 15, 2019.*
Copyright license agreement: *The Copyright License Agreement has been signed by all authors before publication.*
Data sharing statement: *Datasets analyzed during the current study are available from the corresponding author on reasonable request.*
Plagiarism check: *Checked twice by iThenticate.*
Peer review: *Externally peer reviewed.*

References

Arrich J, Holzer M, Havel C, Müllner M, Herkner H (2016) Hypothermia for neuroprotection in adults after cardiopulmonary resuscitation. Cochrane Database Syst Rev 2:CD004128.
Boly M, Massimini M, Tsuchiya N, Postle BR, Koch C, Tononi G (2017) Are the neural correlates of consciousness in the front or in the back of the cerebral cortex? Clinical and neuroimaging evidence. J Neurosci 37:9603-9613.

Burruss JW, Chacko RC (1999) Episodically remitting akinetic mutism following subarachnoid hemorrhage. J Neuropsychiatry Clin Neurosci 11:100-102.
Caballero Perea B, Villegas AC, Rodríguez JM, Velloso MJ, Vicente AM, Cabrerizo CH, López RM, Romasanta LA, Beltrán MS (2012) Recommendations of the Spanish Societies of Radiation Oncology (SEOR), Nuclear Medicine & Molecular Imaging (SEMNiM), and Medical Physics (SEFM) on (18)F-FDG PET-CT for radiotherapy treatment planning. Reports of practical oncology and radiotherapy : journal of Greatpoland Cancer Center in Poznan and Polish Society of Radiation Oncology 17:298-318.
Carlin JL, Jain S, Gizewski E, Wan TC, Tosh DK, Xiao C, Auchampach JA, Jacobson KA, Gavrilova O, Reitman ML (2017) Hypothermia in mouse is caused by adenosine A(1) and A(3) receptor agonists and AMP via three distinct mechanisms. Neuropharmacology 114:101-113.
Casteels C, Vermaelen P, Nuyts J, Van Der Linden A, Baekelandt V, Mortelmans L, Bormans G, Van Laere K (2006) Construction and evaluation of multitracer small-animal PET probabilistic atlases for voxel-based functional mapping of the rat brain. J Nucl Med 47:1858-1866.
Cheong JL, Coleman L, Hunt RW, Lee KJ, Doyle LW, Inder TE, Jacobs SE (2012) Prognostic utility of magnetic resonance imaging in neonatal hypoxic-ischemic encephalopathy: substudy of a randomized trial. Arch Pediatr Adolesc Med 166:634-640.
Crone JS, Soddu A, Höller Y, Vanhaudenhuyse A, Schurz M, Bergmann J, Schmid E, Trinka E, Laureys S, Kronbichler M (2014) Altered network properties of the fronto-parietal network and the thalamus in impaired consciousness. Neuroimage Clin 4:240-248.
Font-Belmonte E, González-Rodríguez P, Fernández-López A (2020) Necroptosis in global cerebral ischemia: a role for endoplasmic reticulum stress. Neural Regen Res 15:455-456.
Forgacs PB, Fridman EA, Goldfine AM, Schiff ND (2016) Isolation syndrome after cardiac arrest and therapeutic hypothermia. Front Neurosci 10:259.
Fridman EA, Beattie BJ, Broft A, Laureys S, Schiff ND (2014) Regional cerebral metabolic patterns demonstrate the role of anterior forebrain mesocircuit dysfunction in the severely injured brain. Proc Natl Acad Sci U S A 111:6473-6478.
Granato A, Santarelli M, Sbriccoli A, Minciacchi D (1995) Multifaceted alterations of the thalamo-cortico-thalamic loop in adult rats prenatally exposed to ethanol. Anat Embryol (Berl) 191:11-23.
Han HS, Park J, Kim JH, Suk K (2012) Molecular and cellular pathways as a target of therapeutic hypothermia: pharmacological aspect. Curr Neuropharmacol 10:80-87.
Kowalik R, Szczerba E, Kołtowski Ł, Grabowski M, Chojnacka K, Golecki W, Hołubek A, Opolski G (2014) Cardiac arrest survivors treated with or without mild therapeutic hypothermia: performance status and quality of life assessment. Scand J Trauma Resusc Emerg Med 22:76.
Lally PJ, Montaldo P, Oliveira V, Soe A, Swamy R, Bassett P, Mendoza J, Atreja G, Kariholu U, Pattnayak S, Sashikumar P, Harizaj H, Mitchell M, Ganesh V, Harigopal S, Dixon J, English P, Clarke P, Muthukumar P, Satodia P, et al. (2019) Magnetic resonance spectroscopy assessment of brain injury after moderate hypothermia in neonatal encephalopathy: a prospective multicentre cohort study. Lancet Neurol 18:35-45.
Lammi MH, Smith VH, Tate RL, Taylor CM (2005) The minimally conscious state and recovery potential: a follow-up study 2 to 5 years after traumatic brain injury. Arch Phys Med Rehabil 86:746-754.
Lant ND, Gonzalez-Lara LE, Owen AM, Fernández-Espejo D (2016) Relationship between the anterior forebrain mesocircuit and the default mode network in the structural bases of disorders of consciousness. Neuroimage Clin 10:27-35.
Larribau R, Deham H, Niquille M, Sarasin FP (2018) Improvement of out-of-hospital cardiac arrest survival rate after implementation of the 2010 resuscitation guidelines. PLoS One 13:e0204169.
Lauritzen KH, Hasan-Olive MM, Regnell CE, Kleppa L, Scheibye-Knudsen M, Gjedde A, Klungland A, Bohr VA, Storm-Mathisen J, Bergersen LH (2016) A ketogenic diet accelerates neurodegeneration in mice with induced mitochondrial DNA toxicity in the forebrain. Neurobiol Aging 48:34-47.
Legriel S, Lemiale V, Schenck M, Chelly J, Laurent V, Daviaud F, Srairi M, Hamdi A, Geri G, Rossignol T, Hilly-Ginoux J, Boisramé-Helms J, Louart B, Malissin I, Mongardon N, Planquette B, Thirion M, Merceron S, Canet E, Pico F, et al. (2016) Hypothermia for neuroprotection in convulsive status epilepticus. N Engl J Med 375:2457-2467.
Li X, Zhu H, Sun X, Zuo F, Lei J, Wang Z, Bao X, Wang R (2016) Human neural stem cell transplantation rescues cognitive defects in APP/PS1 model of Alzheimer's disease by enhancing neuronal connectivity and metabolic activity. Front Aging Neurosci 8:282.
Liang S, Wu S, Huang Q, Duan S, Liu H, Li Y, Zhao S, Nie B, Shan B (2017) Rat brain digital stereotaxic white matter atlas with fine tract delineation in Paxinos space and its automated applications in DTI data analysis. Magn Reson Imaging 43:122-128.
Liu J, Wang Y, Zhuang Q, Chen M, Wang Y, Hou L, Han F (2016) Protective effects of cyclosporine A and hypothermia on neuronal mitochondria in a rat asphyxial cardiac arrest model. Am J Emerg Med 34:1080-1085.
Macniven JA, Poz R, Bainbridge K, Gracey F, Wilson BA (2003) Emotional adjustment following cognitive recovery from 'persistent vegetative state': psychological and personal perspectives. Brain Inj 17:525-533.
Mangin JF, Lebenberg J, Lefranc S, Labra N, Auzias G, Labit M, Guevara M, Mohlberg H, Roca P, Guevara P, Dubois J, Leroy F, Dehaene-Lambertz G, Cachia A, Dickscheid T, Coulon O, Poupon C, Rivière D, Amunts K, Sun ZY (2016) Spatial normalization of brain images and beyond. Med Image Anal 33:127-133.
Massaro AN, Bouyssi-Kobar M, Chang T, Vezina LG, du Plessis AJ, Limperopoulos C (2013) Brain perfusion in encephalopathic newborns after therapeutic hypothermia. AJNR Am J Neuroradiol 34:1649-1655.
McMillan TM, Herbert CM (2004) Further recovery in a potential treatment withdrawal case 10 years after brain injury. Brain Inj 18:935-940.
Monti MM, Rosenberg M, Finoia P, Kamau E, Pickard JD, Owen AM (2015) Thalamo-frontal connectivity mediates top-down cognitive functions in disorders of consciousness. Neurology 84:167-173.
Mooney MR, Unger BT, Boland LL, Burke MN, Kebed KY, Graham KJ, Henry TD, Katsiyiannis WT, Satterlee PA, Sendelbach S, Hodges JS, Parham WM (2011) Therapeutic hypothermia after out-of-hospital cardiac arrest: evaluation of a regional system to increase access to cooling. Circulation 124:206-214.
Neske GT (2015) The Slow oscillation in cortical and thalamic networks: Mechanisms and functions. Front Neural Circuits 9:88.
Nguyen PL, Alreshaid L, Poblete RA, Konye G, Marehbian J, Sung G (2018) Targeted temperature management and multimodality monitoring of comatose patients after cardiac arrest. Front Neurol 9:768.
Nie B, Liu H, Chen K, Jiang X, Shan B (2014) A statistical parametric mapping toolbox used for voxel-wise analysis of FDG-PET images of rat brain. PLoS One 9:e108295.
Nie B, Hui J, Wang L, Chai P, Gao J, Liu S, Zhang Z, Shan B, Zhao S (2010) Automatic method for tracing regions of interest in rat brain magnetic resonance imaging studies. J Magn Reson Imaging 32:830-835.
Nie B, Chen K, Zhao S, Liu J, Gu X, Yao Q, Hui J, Zhang Z, Teng G, Zhao C, Shan B (2013) A rat brain MRI template with digital stereotaxic atlas of fine anatomical delineations in paxinos space and its automated application in voxel-wise analysis. Hum Brain Mapp 34:1306-1318.
Owen AM, Coleman MR, Boly M, Davis MH, Laureys S, Pickard JD (2006) Detecting awareness in the vegetative state. Science 313:1402.
Park YH, Lee YM, Kim DS, Park J, Suk K, Kim JK, Han HS (2013) Hypothermia enhances induction of protective protein metallothionein under ischemia. J Neuroinflammation 10:21.
Paxinos G, Watson C (2005) The rat brain in stereotaxic coordinates. Compact 6th ed. New York: Academic Press.
Quinn B, Dauer Z, Pandit-Taskar N, Schoder H, Dauer LT (2016) Radiation dosimetry of 18F-FDG PET/CT: incorporating exam-specific parameters in dose estimates. BMC Med Imaging 16:41.
Randhawa VK, Nagpal AD, Lavi S (2015) Out-of-hospital cardiac arrest and acute coronary syndromes: reviewing post-resuscitation care strategies. Can J Cardiol 31:1477-1480.
Rutherford M, Ramenghi LA, Edwards AD, Brocklehurst P, Halliday H, Levene M, Strohm B, Thoresen M, Whitelaw A, Azzopardi D (2010) Assessment of brain tissue injury after moderate hypothermia in neonates with hypoxic-ischaemic encephalopathy: a nested substudy of a randomised controlled trial. Lancet Neurol 9:39-45.
Schiff ND (2008) Central thalamic contributions to arousal regulation and neurological disorders of consciousness. Ann N Y Acad Sci 1129:105-118.
Schiff ND (2010) Recovery of consciousness after brain injury: a mesocircuit hypothesis. Trends Neurosci 33:1-9.
Shankaran S, Barnes PD, Hintz SR, Laptook AR, Zaterka-Baxter KM, McDonald SA, Ehrenkranz RA, Walsh MC, Tyson JE, Donovan EF, Goldberg RN, Bara R, Das A, Finer NN, Sanchez PJ, Poindexter BB, Van Meurs KP, Carlo WA, Stoll BJ, Duara S, et al. (2012) Brain injury following trial of hypothermia for neonatal hypoxic-ischaemic encephalopathy. Arch Dis Child Fetal Neonatal Ed 97:F398-404.
Smith ML, Auer RN, Siesjö BK (1984) The density and distribution of ischemic brain injury in the rat following 2-10 min of forebrain ischemia. Acta Neuropathol 64:319-332.
Song M, Zhang Y, Cui Y, Yang Y, Jiang T (2018) Brain network studies in chronic disorders of consciousness: advances and perspectives. Neurosci Bull 34:592-604.
Tang YN, Zhang GF, Chen HL, Sun XP, Qin WW, Shi F, Sun LX, Xu XN, Wang MS (2020) Selective brain hypothermia-induced neuroprotection against focal cerebral ischemia/reperfusion injury is associated with Fis1 inhibition. Neural Regen Res 15:903-911.
Voss HU, Uluğ AM, Dyke JP, Watts R, Kobylarz EJ, McCandliss BD, Heier LA, Beattie BJ, Hamacher KA, Vallabhajosula S, Goldsmith SJ, Ballon D, Giacino JT, Schiff ND (2006) Possible axonal regrowth in late recovery from the minimally conscious state. J Clin Invest 116:2005-2011.
Wang X, You Z, Zhao G, Wang T (2018) MicroRNA-194-5p levels decrease during deep hypothermic circulatory arrest. Sci Rep 8:14044.
Wu TC, Grotta JC (2013) Hypothermia for acute ischaemic stroke. Lancet Neurol 12:275-284.
Wu YW, Mathur AM, Chang T, McKinstry RC, Mulkey SB, Mayock DE, Van Meurs KP, Rogers EE, Gonzalez FF, Comstock BA, Juul SE, Msall ME, Bonifacio SL, Glass HC, Massaro AN, Dong L, Tan KW, Heagerty PJ, Ballard RA (2016) High-dose erythropoietin and hypothermia for hypoxic-ischemic encephalopathy: a phase ii trial. Pediatrics 137:e20160191.
Zhang F, Guo A, Liu C, Comb M, Hu B (2013) Phosphorylation and assembly of glutamate receptors after brain ischemia. Stroke 44:170-176.
Zhang J, Zou H, Zhang Q, Wang L, Lei J, Wang Y, Ouyang J, Zhang Y, Zhao H (2016) Effects of Xiaoshuan enteric-coated capsule on neurovascular functions assessed by quantitative multiparametric MRI in a rat model of permanent cerebral ischemia. BMC Complement Altern Med 16:198.

C-Editor: Zhao M; S-Editors: Yu J, Li CH; L-Editors: Dawes EA, Song LP; T-Editor: Jia Y